

# Measurement of $t\bar{t}$ Cross Section in the Lepton Plus Jets Channel Using Neural Networks in $4.6\text{ fb}^{-1}$ , Including the Ratio Over the Z Cross Section $fb^{-1}$

**A. Lister**

*University of Geneva*

**J. Conway, R. Erbacher, W. Johnson, T. Schwarz**

*University of California at Davis*

**K. Lannon,**

*University of Notre Dame*

**R. Hughes, B. Winer**

*The Ohio State University*

CDF NOTE xxxx

Version 0.0

July 27, 2009

## Abstract

We present here an update the measurement of the  $p\bar{p} \rightarrow t\bar{t}$  cross section in the lepton+jets channel using kinematics in  $4.6\text{ fb}^{-1}$  of CDF data (corresponding to data up to period 23). The changes with respect to the previous iteration of this analysis, that used  $2.8\text{ fb}^{-1}$  are four things. The first is the use of more data. The second is the use of the new Monte Carlo generated with a good run list corresponding to a higher luminosity profile, for both the signal and the W+jets background. The third is a shift of the central value of the top mass from  $175\text{ GeV}/c^2$  to  $172.5\text{ GeV}/c^2$ , the cross section is also quoted for 2 other mass points, 170 and  $175\text{ GeV}/c^2$ . The final change is the use of a cut in angular separation, in  $\phi$ , between the muon and the missing transverse energy at 3.05, as used in the  $t'$  searches; this cut removes the mis-measured muons that appear to have very high  $p_T$ .

We obtain a  $t\bar{t}$  cross section of  $XX \pm XX$  (stat)  $\pm XX$  (sys) pb for this direct measurement including all three lepton types (CEM, CMUP, CMX). Separating out explicitly the luminosity from the other systematics, we obtain  $\sigma_{t\bar{t}} = XX \pm XX$  (stat)  $\pm XX$  (sys)  $\pm XX$  (lumi) pb. Furthermore, as for the last analysis, we consider the ratio of the top to the Z cross section using only the CEM electrons and CMUP muons. The cross section, using this method, is measured to be  $YY \pm YY$  (stat)  $\pm YY$  (sys)  $\pm YY$  (theory) pb. The total uncertainty on the measured top cross section is now ZZ %.

# 1 Introduction

The purpose of this note is to update the kinematic  $t\bar{t}$  cross section measurement using the latest version of the Top Group software and the larger dataset currently available. We have repeated the procedures used in the previous round of this analysis using the new data and a few minor changes described below. In this analysis we use a feed forward NN with seven inputs, one hidden layer having seven nodes and one output. The shape of the NN output distribution, obtained after processing our standard Monte Carlo (MC) samples with the trained network, is used as the final discriminating variable. A binned maximum likelihood fit to the data events is performed and the  $t\bar{t}$  cross section is extracted from a  $4.6 fb^{-1}$  data set. The previous iteration of this analysis, using  $2.8 fb^{-1}$ , can be found in [1] [2] for the default and the ratio over the Z cross section, respectively. Prior iterations of the analysis, that only use the direct measurement, can be found in [3] [4] [5]. Measuring the  $t\bar{t}$  cross section in the lepton+jets channel using kinematic and event shape variables takes advantage of a larger data set and nicely compliments the b-tag analysis. While the b-tagged analysis has to contend with larger systematics due to the understanding of the b-tagging and of heavy flavour, this analysis is more dependent on the correct description of the kinematics of the event. Nonetheless, care was taken when choosing the NN input variables, to consider only kinematic quantities we believe to be well modelled by our Monte Carlo.

Below is a description of the changes between this update and the previous version.

- Add data up to p23 that corresponds to  $4.6 fb^{-1}$  of data.
- Use new Monte Carlo generated using a good run list corresponding to a higher luminosity profile.
- A new central value for the assumed top mass is chosen:  $172.5 \text{ GeV}/c^2$  instead of  $175 \text{ GeV}/c^2$ . Other mass points are also considered:  $170 \text{ GeV}/c^2$  and  $175 \text{ GeV}/c^2$ .
- The use of a cut in angular separation, in  $\phi$ , between the muon and the missing transverse energy at 3.05, as used in the  $t'$  searches; this cut removes the mis-measured muons that appear to have very high  $p_T$ .
- Use good run list v29 with no silicon.
- Use jetCorr18 for jet energy corrections.
- Update trigger efficiencies, ID and reconstruction scale factors as well as Zvtx scale factors.

## 2 Data Sample

We are using the official Top Group high  $p_T$  lepton data-sets **bhelxx** and **bhmuxx**. The event selection and analysis are done in the 6.1.4 off-line release. The event selection used is the default top group lepton + jets selection except for the QCD removal cuts which are optimised for this analysis and the  $\Delta\phi$  cut to remove mis-measured muons.

Good quality requirements are enforced by v29 of the DQM good run list [13] with no silicon requirements. The total luminosity considered for each trigger is shown in Tabl 1. The uncertainty on the integrated luminosity is taken to be 5.8% [14].

	CEM	CMUP	CMX
Lumi [ $pb^{-1}$ ]	4597.73	4588.41	4532.28

Table 1: Total integrated luminosity for the sample considered.

### 3 Signal and Background Simulation

Official Top group 6.1.4mc Monte Carlo samples and public Top Lepton+Jets group Top-Ntuples of these samples were used in this analysis [15]. Signal  $t\bar{t}$  samples were generated with both PYTHIA and HERWIG. The PYTHIA sample is used as the nominal signal model while HERWIG is used to evaluate a systematic error on the signal modelling. The dominant background from  $W$ +jets was modelled with the leading order W+N parton matrix element generator ALPGEN interfaced to the parton shower from PYTHIA. The new parton matching scheme is used in order to model the whole spectrum of W+jets. The NN have been trained using only the relevant parton. For example the  $\geq 4$  jet NN is trained using only the W+4p sample. The final fit is carried out using the whole merged spectrum. Other backgrounds like  $Z$ +jets,  $WW$ +jets,  $WZ$ +jets,  $ZZ$ +jets were also modelled with ALPGEN.

The background from QCD multi-jets is difficult to model with MC. Therefore, we model this background from the data. For this iteration of the analysis, the jet-electrons are again used as the nominal sample, with the anti-electrons being considered for an estimate of the systematic. This is the same as was done for the previous iteration. The QCD cuts have not been changed. Note that we added more data to the QCD samples in the same way as we add data for the analysis.

### 4 Event Selection

We follow the standard lepton + jets event selection as detailed in [12]. A brief overview of the selection is given below.

We use the electron and muon definitions established by the W and Z cross section groups in this analysis. We use CEM electrons and CMUP and CMX muons only. Given that all of our events must include, by definition, a high-momentum electron or muon, the data sample should only contain events that came in on CEM, CMUP or CMX triggers. The requirement that the lepton came in on the appropriate trigger is made.

To clean up the sample, electron events in which the primary electron is identified as a conversion are removed. Similarly, muon events containing a cosmic ray are removed. Signal events should contain only one high- $p_T$  lepton. We veto events consistent with a leptonic  $Z$  decay.

The same jet clustering algorithm, JETCLU with cone of 0.4, and jet selection criteria,  $E_T > 20$  GeV and  $|\eta| < 2.0$ , is used as in previous versions of this analysis. Moreover, we select events after jet corrections have been made up to and including level 5 in order to flatten calorimeter response. The  $\cancel{E}_T$  is corrected for the muon  $p_T$  in including the effect of muon curvature corrections.

In order to ensure the jets and lepton are reconstructed from the same interaction, we require that the event z vertex position, as defined by the closest good quality ZVertexModule object (quality  $\geq 12$ ) to be within 5 cm of the tight lepton  $z_0$ .

To reduce the QCD fakes background, we require some additional cuts described in detail in the note for the previous analysis: Missing transverse energy  $\geq 35$  GeV, leading jet  $E_T \geq 35$  GeV.

## 4.1 Data events

Table 2 contains the number of observed events in the data as a function of reconstructed jet multiplicity bins of interest. All of the selection criteria described above have been applied. The data is broken out in terms of electron+jets and muon+jets. For comparison, the number of expected  $t\bar{t}$  events is also presented based on an assumed cross section of 7.45 pb.

Njets	CEM	CMUP	CMX	Total	Expected $t\bar{t}$ (7.45 pb)
3	3810	1666	928	6404	888
$\geq 4$	1309	563	347	2219	1093
$\geq 3$	5119	2229	1275	8623	1981

Table 2: The number of events selected for this analysis. For the  $t\bar{t}$  expectation, a cross section of 7.45 pb is assumed for a mass of 172.5 GeV/c<sup>2</sup>.

## 5 Kinematic variables

The main background to  $t\bar{t}$  production in the lepton+jets channel comes from  $W$  production associated with hadronic jets. The contribution from QCD-fakes background, falls off rather fast with the missing energy and generally is assumed to populate less energetic regions of the phase space. The selection of the discriminating variables and training the NN is focused on trying to achieve good separation between  $t\bar{t}$  and  $W + np$  events. The additional backgrounds will be later taken into account in the final fit as well as the associated systematics.

The variables used in this analysis to discriminate between  $t\bar{t}$  and  $W$ +jets fall into two categories: kinematic and event shape. Both types of variables have advantages in separating  $t\bar{t}$  from the  $W$ +jets background. Due to the large mass of the top quark,  $t\bar{t}$  events tend to be more energetic than background processes. As a result energy based kinematic variable have good discriminating power for separating  $t\bar{t}$  events. Since  $t\bar{t}$  events are expected to be more spherical than the  $W$ +jets, event shape variables, like aplanarity or sphericity, can be useful. In addition, because of the large top quark mass,  $t\bar{t}$  events tend to be more central, making variables involving jet pseudo-rapidities useful. The exact combination of kinematic and event shape variables used for this analysis was chosen based on the extensive studies documented in CDF Note 6897 [5]. In the end, the following set of variables was chosen based on the statistical sensitivity and systematic error the combination was able to achieve in pseudo-experiments (in order of expected sensitivity based on fits with single variables):

- $EtJ_{345}$  is the scalar sum of the jet  $E_T$  for third through fifth highest  $E_T$  tight jets in the event.
- $H_T$  is the scalar sum of the transverse energies of the five highest  $E_T$  tight jets, the lepton, and the  $\cancel{E}_T$ .
- $SumEz/SumEt$  is the scalar sum of the  $z$ -component of the momentum for the five highest  $E_T$  tight jets divided by the scalar sum of the  $E_T$  of these same jets.
- $MinDijetMass$  is the minimum dijet invariant mass from among the three highest  $E_T$  jets.
- $MaxJetRapidity$  is the maximum jet eta from among the three highest  $E_T$  jets.
- $Aplanarity$  is constructed using the lowest eigenvalue ( $Q_1 \leq Q_2 \leq Q_3$ ) of the normalised momentum tensor as follows:

$$Aplanarity = 3/2 Q_1 \quad (1)$$

The momentum tensor is constructed using up to 5 highest  $E_T$  tight jets, lepton momentum and transverse missing energy. No reconstruction of  $P_z$ , the  $z$  momentum component of the neutrino from the  $W \rightarrow l\nu$  decay is attempted.

- $MinDijetSeparation$  is the minimum separation  $\Delta R = \sqrt{\Delta\eta^2 + \Delta\phi^2}$

Table 3 shows the expected sensitivity, based on 10'000 pseudo-experiments (PE) of the 7 different input variables and the final NN output discriminant. The last column shows the number of PEs for which the MINOS error did not find convergence; note that in all cases a minimum was found, but no error calculation was possible, leading to the assumption that the minimum was not well defined. This last column shows that not a single variable could reliably be used to extract the top cross section

Variable	Expected Sensitivity	Number PE failed
Sum $E_T$ jets 3,4,5	0.30	1023
$H_T$	0.34	1757
Min Dijet Mass	0.71	186
$SumEz/SumEt$	0.74	1
Maximum $\eta$	0.79	913
Min Dijet Separation	1.10	4969
Aplanarity	1.42	7027
NN output	0.32	0

Table 3: Expected sensitivity of each input variable to the NN when considered alone along with the expected sensitivity for the NN output distribution. The right column shows the number of PE where MINOS failed to find errors.

## 6 The use of NN for classification problems

*this section is unchanged with respect to the previous version and the NN has not been retrained.*

For NN training we use JETNET [16] package, developed at CERN and the RootJetnet interface developed by CDF [17]. The NN will have seven input variables, one hidden layer and one continuous output unit in the range [0,1].

For our purpose here, a convenient way to look at a NN would be as a mapping function between the input variable space to the output variable space designed to realise maximum output separation between signal and background events. It is known that by increasing the number of hidden nodes a NN having one single layer can approximate any arbitrary mapping having finite discontinuities from the the input space to the output space [18]. By choosing a small number of input variables we effectively project the problem in a space of much lower dimensionality within which an approximation of the mapping can be found using a modest number of hidden units.

JETNET implements a variety of training algorithms. The training process is designed to minimise the error function defined as a sum over events in the training sample:  $E = \sum_i (NN_{out}(i) - target(i))^2$ . For this particular problem we get satisfactory results using the default back-propagation method with momentum ( $\alpha$ ) added in order to improve learning stability at the end of training. Learning is performed by modifying the network weights ( $\omega$ ) in order to minimise the error function:

$$\Delta\omega_{t+1} = -\eta \frac{\partial E}{\partial \omega} + \alpha \Delta\omega_t \quad (2)$$

We use the default JETNET learning rate  $\eta = .001$ , momentum  $\alpha = 0.5$ . Ten different patterns are being probed before an update of the weights is performed. In principle all these parameters as well as the training algorithm can be varied but we did not see any significant improvement in NN performance.

CDF Note 6897 documents extensive studies performed to determine the optimal number of nodes in the input and hidden layers of the neural net. In updating this measurement, we rely on the results of these studies to determine the structure of the network we use.

## 7 Normalisation of the QCD Background

The normalisation of the QCD background is determined using the standard  $\cancel{E}_T$  fit method. The QCD background dominates at low  $\cancel{E}_T$  and the spectrum is expected to fall off rapidly with increasing  $\cancel{E}_T$ . All final event selection cuts are applied except for the  $\cancel{E}_T$  cut.

A fit, using TFractionFitter, is carried out with the top cross-section fixed at  $7.45 \text{ pb} \pm 7\%$  corresponding to the theoretical uncertainty. The number of QCD events is floated. The number of W+jets events is defined to be everything that is not top and not QCD. The fit is carried out in 40 bins covering a range from 0-200 GeV, the overflow bins is added to the final bin.

After the  $\cancel{E}_T$  fit, the  $\cancel{E}_T$  cut is applied and the expected number of QCD events is determined. In the final fit to the NN output distribution, the number of QCD events is left to float within  $\pm 50\%$  of this nominal value.

The fitted number of QCD events are shown in Table 4 both before and after the final MET cut. As an example the fit the  $\cancel{E}_T$  is shown in Figures 1 and 2 for the jet electron QCD model and the anti-electron QCD model, respectively.

It is apparent from this table that the numbers obtained from both the jet-electron and the non-isolated leptons are very similar to each other before any missing transverse energy cut is applied. One important cross-check is that sum of the values for each trigger should roughly

equal the fitted value considering all triggers in a single set of templates. This shows that there is no bias in the fit due to the separation among triggers or not. The maximum difference in the fitted event numbers between the two QCD models is of the order of 50% which is the constraint we place on the number of QCD events in the final fit and also the systematic shift we apply in the starting point for the final fit.

	CEM	CMX	CMUP	Total
$\geq 3$ jets				
Jet-electron Sample				
Before $\cancel{E}_T$ cut	12702 $\pm$ 336	824.817 $\pm$ 88	668 $\pm$ 69	14423 $\pm$ 418
After $\cancel{E}_T$ cut at 35 GeV	394	26	21	448
Anti-electron Sample				
Before $\cancel{E}_T$ cut	12982 $\pm$ 6231	777 $\pm$ 96	640 $\pm$ 78	14520 $\pm$ 612
After $\cancel{E}_T$ cut at 35 GeV	694	42	34	777
3 jets				
Jet-electron Sample				
Before $\cancel{E}_T$ cut	10707 $\pm$ 602	703 $\pm$ 85	617 $\pm$ 626	12234 $\pm$ 392
After $\cancel{E}_T$ cut at 35 GeV	310	20	18	354
Anti-electron Sample				
Before $\cancel{E}_T$ cut	10957 $\pm$ 476	664 $\pm$ 95	587 $\pm$ 75	12285 $\pm$ 575
After $\cancel{E}_T$ cut at 35 GeV	538	33	29	603
$\geq 4$ jets				
Jet-electron Sample				
Before $\cancel{E}_T$ cut	1967 $\pm$ 205	99 $\pm$ 34	46 $\pm$ 32	2159 $\pm$ 136
After $\cancel{E}_T$ cut at 35 GeV	85	4	11	2
Anti-electron Sample				
Before $\cancel{E}_T$ cut	2030 $\pm$ 1237	91 $\pm$ 21	43 $\pm$ 32	2174 $\pm$ 174
After $\cancel{E}_T$ cut at 35 GeV	168	8	4	180

Table 4: The contribution to the data from the QCD background using the jet-electron and anti-electron QCD models both before and after the  $\cancel{E}_T$  cut at 35 GeV. The errors are the statistical (data + template) errors returned by TFractionFitter.

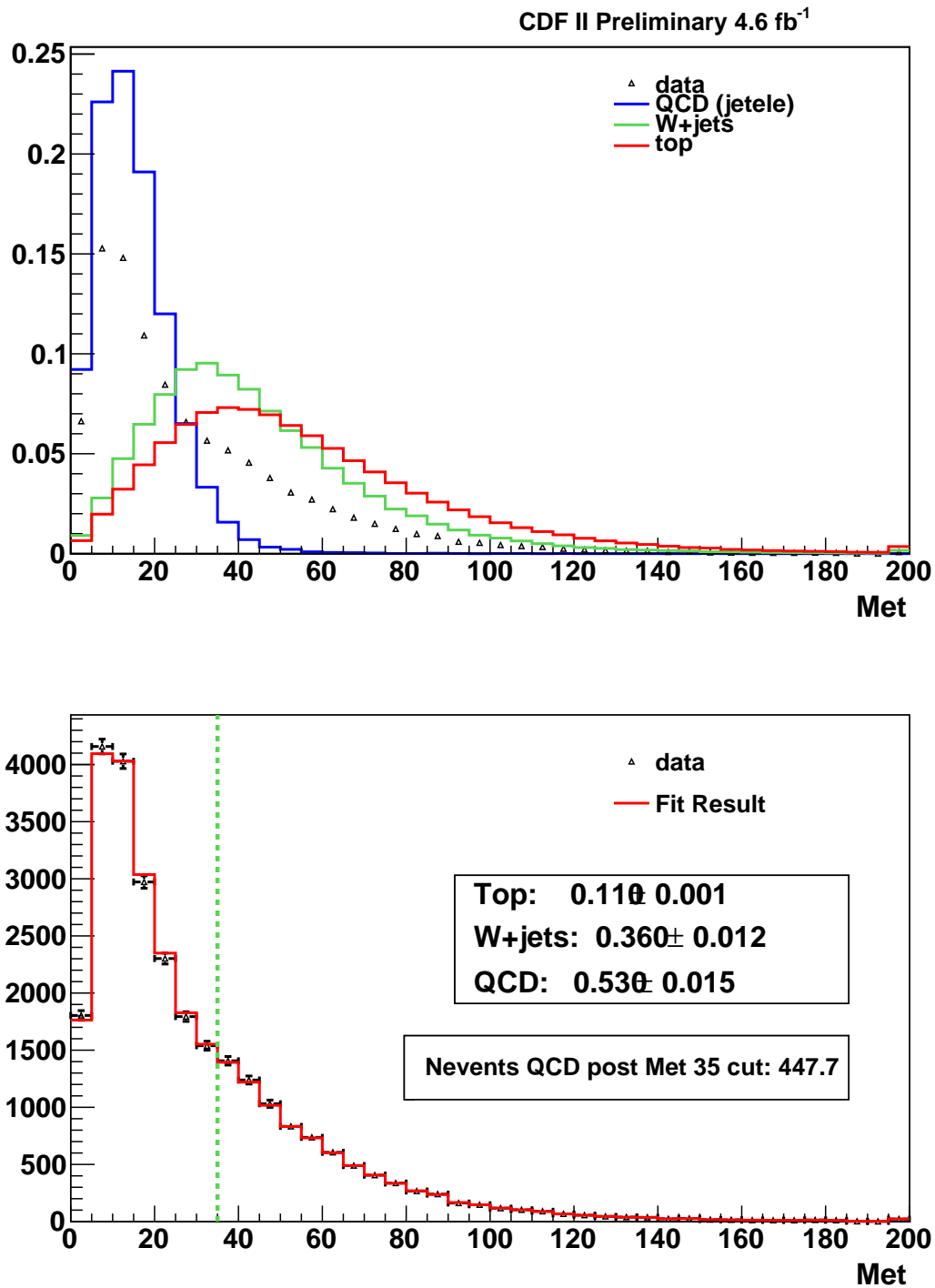


Figure 1: (top)  $\cancel{E}_T$  templates for the data, top signal, W+jets and QCD backgrounds in the W+ $\geq 3$  jet case. The QCD model used here is jet-electrons. These plots are normalised to unit area. (bottom) Comparison between the data and the fitted distribution.



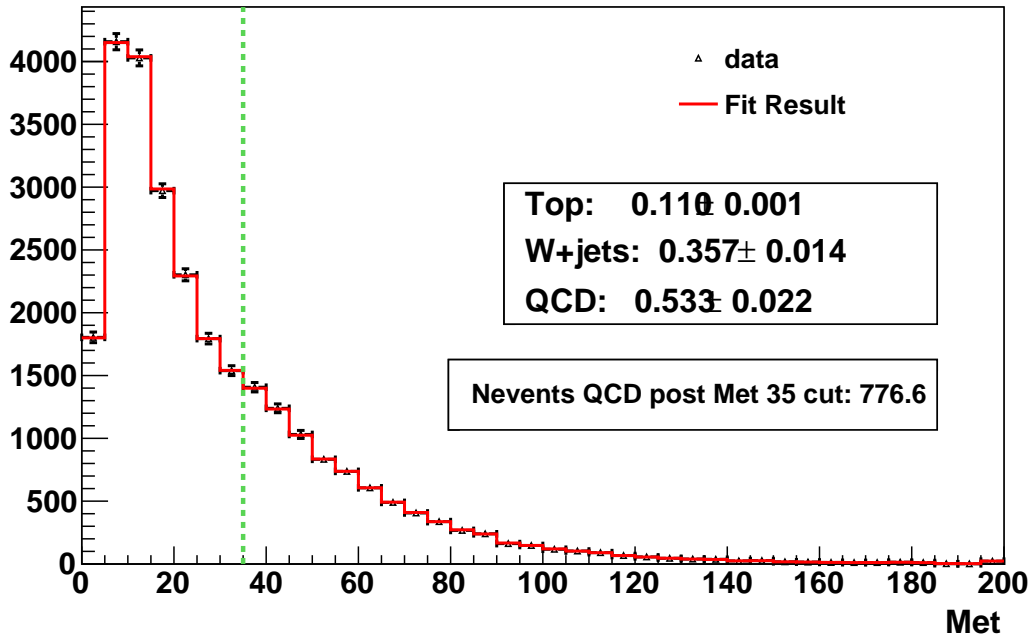
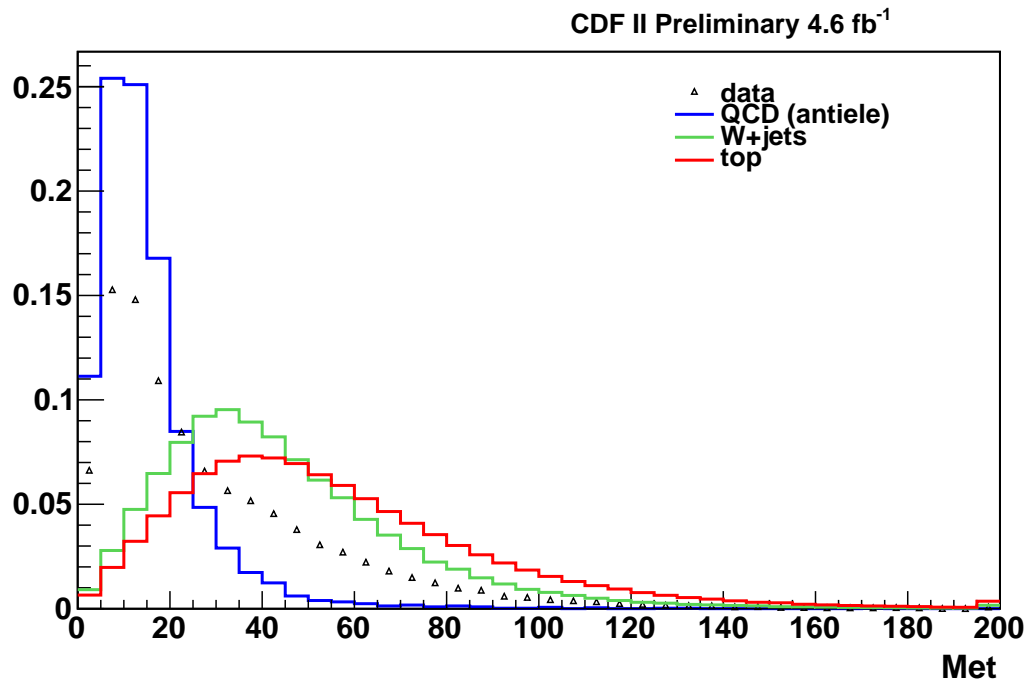


Figure 2: (top)  $\cancel{E}_T$  templates for the data, top signal, W+jets and QCD backgrounds in the W+ $\geq 3$  jet case. The QCD model used here is anti-electrons. These plots are normalised to unit area. (bottom) Comparison between the data and the fitted distribution.

## 8 Top Acceptance

The cross-section for  $t\bar{t}$  production is defined based on the following formula.

$$\sigma_{t\bar{t}} = \frac{N_{t\bar{t}}}{\sum_{\text{trig}} A_{\text{trig}}(t\bar{t}) \cdot \mathcal{L}_{\text{trig}}}, \quad (3)$$

where  $N_{t\bar{t}}$  is the number of observed top events in the data,  $\sigma_{t\bar{t}}$  is the  $t\bar{t}$  cross-section that we wish to fit for,  $\mathcal{L}_{\text{trig}}$  is the integrated luminosity, and  $A$  is the acceptance. The denominator can be written out explicitly in the following form:

$$\sum_{\text{trig}} A_{\text{trig}}(t\bar{t}) \cdot \mathcal{L}_{\text{trig}} = [\varepsilon_{\text{cmx}}^{\text{trigger}}(t\bar{t}) \cdot SF_{\text{cmx}}^{\text{IDreco}}(t\bar{t}) \cdot A_{\text{cmx}}^{\text{MC}}(t\bar{t}) \cdot \mathcal{L}_{\text{cmx}} \quad (4)$$

$$+ \varepsilon_{\text{cmup}}^{\text{trigger}}(t\bar{t}) \cdot SF_{\text{cmup}}^{\text{IDreco}}(t\bar{t}) \cdot A_{\text{cmup}}^{\text{MC}}(t\bar{t}) \cdot \mathcal{L}_{\text{cmup}} \\ + \varepsilon_{\text{cem}}^{\text{trigger}}(t\bar{t}) \cdot SF_{\text{cem}}^{\text{IDreco}}(t\bar{t}) \cdot A_{\text{cem}}^{\text{MC}}(t\bar{t}) \cdot \mathcal{L}_{\text{cem}}] \cdot SF_{Z_{\text{vtx}}}, \quad (5)$$

where  $\varepsilon^{\text{trig}}(t\bar{t})$  is the trigger efficiency for that particular trigger,  $SF^{\text{IDreco}}(t\bar{t})$  is the data / MC scale factor for the lepton identification and reconstruction and  $A^{\text{MC}}(t\bar{t})$  is the  $t\bar{t}$  acceptance in MC. These numbers are computed separately for each trigger.  $SF_{Z_{\text{vtx}}}$  is the  $Z_{\text{vtx}}$  scale factor to account for the small difference in the total acceptance due to the effect of applying the  $|Z_{\text{vtx}}| < 60$  cm cut. This SF has only a very small effect on the overall acceptance.

The values for  $\varepsilon^{\text{trig}}(t\bar{t})$  and  $SF^{\text{IDreco}}(t\bar{t})$  are calculated from the Joint Physics method and spreadsheet [21] where the individual numbers are obtained using Perfidia [22]. The  $SF_{Z_{\text{vtx}}}$  is computed using the numbers for from JointPhysics given that the  $Z_{\text{vtx}}$  efficiency is 1 in MC as we compute the number of generated events after the cut is applied.  $A^{\text{MC}}(t\bar{t})$  is computed from the  $t\bar{t}$  MC (ttop25 for nominal value) as the ratio of  $\frac{n_{\text{acc}}}{n_{\text{gen}}}$ .

The numbers for each of the quantities in equation 5 are listed for reference in Table 5.

## 9 Data vs Monte Carlo Comparisons

The reader is requested to refer to [http://www-cdf.fnal.gov/internal/people/links/AlisonLister/topXs/data\\_validation/p17\\_p23/dataMcComp.shtml](http://www-cdf.fnal.gov/internal/people/links/AlisonLister/topXs/data_validation/p17_p23/dataMcComp.shtml) for a comprehensive set of data vs MC validation plots for data up to period 23. Along with the plots combining all data, each trigger is separated as well as each jet bin.

## 10 Validation of new MC samples

The MC samples used for this analysis are either new samples (in the case of top mass 172.5) that were generated using a good run list that spans a wide luminosity range, or are a combination of the old MC used in the previous iteration merged with new MC generated with a higher luminosity profile and where the number of generated events, when added to the original sample, resembles that of the data.

It turns out that the data still has a higher number of primary vertices (a reasonable judge of

Variable	Value	Absolute error
$\varepsilon_{cem}^{trigger}(t\bar{t})$	0.962	0.004
$\varepsilon_{cmup}^{trigger}(t\bar{t})$	0.882	0.012
$\varepsilon_{cmx}^{trigger}(t\bar{t})$	0.911	0.010
$SF_{cem}^{IDreco}$	0.977	0.005
$SF_{cmup}^{IDreco}$	0.900	0.008
$SF_{cmx}^{IDreco}$	0.956	0.009
$\geq 3$ jets		
$A_{cem}^{MC}(t\bar{t})$	0.036	
$A_{cmup}^{MC}(t\bar{t})$	0.022	
$A_{cmx}^{MC}(t\bar{t})$	0.010	
$SF_{Z_{vtx}}$	0.971	0.002

Table 5: Acceptance numbers used for this cross section measurement along with the absolute uncertainties.

luminosity profile) than the new MC.

The interested reader is referred to talks, by A. Lister, in the top meeting in June/July 2009 on this subject.

## 11 Cross section calculation

We perform a binned maximum likelihood fit to the NN distribution in the  $W + \geq 3$  jet region. We use PYTHIA  $t\bar{t}$  to model the signal, ALPGEN+PYTHIA  $W + n$  parton to model the  $W + \text{jets}$  background and the jet-electron sample to model the QCD multi-jet background. We constrain the QCD background to **448** events with an uncertainty of **224** events.

In order to test the fitting procedure, we carry out the PEs mentioned in section 5 and test the pull widths and mean which are compatible with 1 and zero, respectively.

## 12 Systematics

The systematics for this analysis have been redone.

100'000 pseudo-experiments (PE) are thrown using the shifted templates (both shape and normalisation are changed when relevant). We fit the PE using nominal templates and nominal acceptance values. Note that for the systematics that affect the  $W + \text{jets}$ , as the normalisation is left to float in the fit, the only systematic effect considered is that of the shape. The systematics affecting the shape of the  $W + \text{jets}$  are: JES and  $Q^2$ . For cases where we have two shifts representing an increase and a decrease of some variable, the systematic is determined as half of the maximal deviation between the three values: nominal, shifted up and shifted down. For the case where the nominal value is between the two shifted templates, the uncertainty is simply given by half the upwards minus the downwards shift. For some of the systematics (IFSR

and  $Q^2$ ) the shift goes in the same direction when increasing and decreasing the parameter. Thus the associated systematic will be half of the difference between the nominal template and the template with the largest shift.

The final measured systematic uncertainties are show in Table 6 .

Effect	Acceptance	Shape	Upwards shift	Downwards shift	Uncertainty
Jet $E_T$ Scale	YES	YES	+3.39	-2.39	2.89
W+jets $Q^2$ Scale	NO	YES	+4.44	+7.61	3.80 (PRELIMINARY!!!)
$t\bar{t}$ IFSR	YES	YES	+0.21	-0.53	
QCD shape	NO	YES			
QCD fraction	YES	NO	-0.89	+0.50	
QCD combined	YES				0.91
$t\bar{t}$ generator	YES	YES			2.72
$t\bar{t}$ branching ratio	YES	YES			Still in progress...
$t\bar{t}$ PDF	YES	NO			
Other EWK	NO	YES			1.0
Color Reconnection	YES	YES	-0.60	-0.43	0.60
CEM ID SF	YES	NO	+0.30	-0.30	0.30
CMUP ID SF	YES	NO	+0.25	-0.25	0.25
CMX ID SF	YES	NO	+0.13	-0.13	0.13
CEM Trigger Efficiency	YES	NO	+0.23	-0.23	0.23
CMUP Trigger Efficiency	YES	NO	+0.38	-0.38	0.38
CMX Trigger Efficiency	YES	NO	+0.16	-0.15	0.15
Zvtx SF	YES	NO	+0.21	-0.21	0.21
Lepton ID/trigger/Zvtx SF	YES	NO	+0.66	-0.66	0.66
Total before Lumi	-	-			
Luminosity	YES	NO	+5.80	-5.80	5.80
Total Systematic	-	-			
Statistical	-	-	+4.45	-4.41	4.43
Total Uncertainty	-	-			

Table 6: Table of the systematic errors for the direct measurement, considering all tight leptons. The overall uncertainty is obtained by adding in quadrature the individual effects.

The effect on both the shape and the acceptance of the various systematics, when applicable are shown in Figures ?? to ??. Only the  $W+\geq 3$  jet bin plots are shown.

Figure ?? shows a comparison between the QCD models considered. The nominal sample used is the jet-electron sample. It is apparent from this plot that the anti-electron model suffers from large statistical fluctuations. The non-isolated leptons are also shown for comparison. The combined sample shown a much smoother behaviour. The systematic is estimated from PE using the the anti-electron sample and fitting to the jet-electron sample. The systematic shift is 0.9%. Note that a similar effect is obtained when simply fitting the data using the

other QCD model (as shown in the NN output plots in the results section).

The QCD fraction systematic is estimated by doubling and halving the constraint on the QCD input normalisation used in the final fit.

Figure ?? shows the effect of shifting the JES up and down by 1 sigma on both the top and the W+jets templates. For the W+jets, only the shape change is shown, the templates are normalised to unit area. This is the largest systematic for the  $W+\geq 4$  jet case.

Figure ?? shows the effect on the top templates of requiring more or less IFSR. This sample is generated by increasing both the initial- and the final-state radiation simultaneously. For this systematic the shift is observed in the same direction for both the IFSR more and IFSR less samples.

Figure ?? shows the effect on the W+jets templates of changing the  $Q^2$  scale up or down by a factor of two. Again, only the shape uncertainty is relevant for this effect. For this systematic the shift is observed in the same direction in both the  $Q^2*2$  and  $Q^2/2$  samples in the  $W+\geq 3$  jet case.

Figure ?? shows the effect on the top templates when using Herwig MC (otop1s) instead of the default Pythia samples (ttkt75). This effect is mostly an acceptance effect that seems to be caused by a different fraction of dilepton events passing our event selection between the two MC samples. Note that we also compared to the htop75 (old JIMMY tune) and the otop02 (no JIMMY) and see the same effect. This systematic is the largest systematic for the  $W+\geq 3$  jet case.

Figure ?? shows in red the nominal top templates along with 46 black curves, each representing a different set of PDF eigenvectors. The different PDFs are generated using the re-weighting technique prescribed by the Joint Physics group. From this plot it is apparent that the shapes are all very similar. For the PDFs we thus only compute and acceptance systematic, obtained using the standard Joint Physics prescription.

The systematic associated with the inclusion of the other EWK backgrounds was not redone for this analysis. The values used here are those used for the previous version of the analysis.

The Lepton ID and reconstruction scale factor as well as the trigger efficiencies are obtained from the Joint Physics Perfidia method. This method also provides the uncertainties on these values for each of the triggers. The uncertainties are combined to form a global Lepton ID+reco + trigger efficiency uncertainty of 0.6%. In a similar way, there is an uncertainty related to the  $Z_{\nu\tau}$  scale factor, also provided by Joint Physics. This uncertainty is small, 0.2%.

Finally, the uncertainty on the luminosity is taken as 5.8% as per the Joint Physics prescription.

The total uncertainty on the measurement is computed by adding all of the uncertainties in quadrature. The total uncertainty is computed both before and after the inclusion of the

luminosity uncertainty. For the most sensitive case,  $W+\geq 3$  jets, the total uncertainty is 6.8% and 9.0% before and after the luminosity, respectively. This corresponds to a total uncertainty on the measured cross-section of 0.46 and 0.61.

## 13 Results

We add all of the systematic uncertainties in quadrature to obtain the final measurement of the top cross-section. The final measured top cross-section for a top mass of 172.5 GeV/c<sup>2</sup> in the  $\geq 3$  jet bin is given by

$$\sigma_{t\bar{t}} = 7.63 \pm 0.43(stat) \pm xx(syst) \pm 0.44(lumi)pb. \quad (6)$$

With our final event selection we have 8623 data events. The final fit tells us that the mean number of events is: 493 QCD events, 6099 W+jets events (i.e. other backgrounds) and 2029  $t\bar{t}$  events.

Figure 3 shows the NN output distribution used for the final fit, as compared to the predictions, based on the normalisations returned by the fit. The KS value of this fit is 98.4%, a good value.

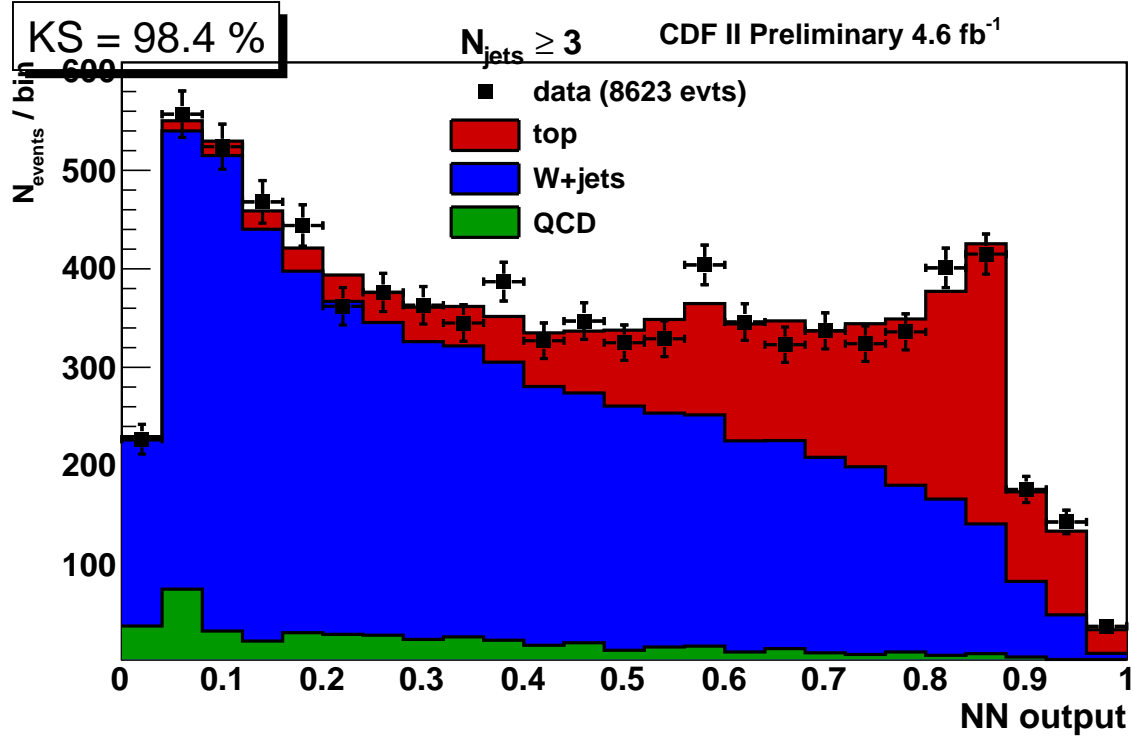


Figure 3: NN output distribution in data (black points) compared to the fitted values for the signal (red) plus background (blue and green for W+jets and QCD, respectively).

## 13.1 Results as a Function of the Assumed Top Mass

Sorry work in progress.....

## 13.2 Ratio of the top to the Z cross section

Sorry work in progress....

# 14 Summary

We presented an update of the measurement of the  $p\bar{p} \rightarrow t\bar{t}$  cross section in the lepton+jets channel. A neural network having kinematic and event shape variables as inputs is used to distinguish the top signal from the W+jets background. NN training was performed on W+np and  $t\bar{t}$  Montecarlo. The shape of the NN output distribution, obtained by processing our standard Montecarlo samples with the trained network, is used as the final discriminating variable. The QCD fakes template was derived from a data sample of jet electrons. Anti-electrons were used to determine the systematics due to the QCD modelling.

We perform a binned maximum likelihood fit to the data and extract a ttbar fraction. From a sample of data corresponding to  $4.6\text{ fb}^{-1}$  of integrated luminosity, the  $t\bar{t}$  cross section is measured to be  $\sigma_{t\bar{t}} = 7.63 \pm 0.43(stat) \pm xx(syst) \pm 0.44(lumi)$  pb assuming a top mass of 172.5 GeV/c. The total uncertainty on this measurement is now xx%.

Conclusions on the ratio to come.....

## References

- [1] J. Conway, R. Erbacher, R. Hughes, K. Lannon, A. Lister, B. Winer *Measurement of the  $t\bar{t}$  Cross Section in the Lepton Plus Jets Channel Using Neural Networks in  $2.8\text{fb}^{-1}$* , CDF Note 9387.
- [2] J. Conway, R. Erbacher, R. Hughes, W. Johnson, K. Lannon, A. Lister, T. Schwarz, B. Winer *ADDENDUM: Measurement of the  $t\bar{t}$  Cross Section in the Lepton Plus Jets Channel Using Neural Networks in  $2.8\text{fb}^{-1}$ . Ratio Over the Z Cross Section*, CDF Note 9528.
- [3] John Conway, Robin Erbacher, Richard Hughes, Kevin Lannon, Rob Roser, Evelyn Thomson, Brian Winer *Measurement of the  $t\bar{t}$  Cross Section in the Lepton Plus Jets Channel using Neural Networks*, CDF Note 8063.
- [4] John Conway, Robin Erbacher, Richard Hughes, Ben Kilminster, Kevin Lannon, Rob Roser, Evelyn Thomson, Brian Winer *Measurement of the  $t\bar{t}$  Cross Section in the Lepton Plus Jets Channel using Neural Networks*, CDF Note 7563.
- [5] Robin Erbacher, Richard Hughes, Radu Marginean, Rob Roser, Evelyn Thomson, Brian Winer John Conway, *Measurement of the  $t\bar{t}$  Cross Section in the Lepton Plus Jets Channel using Neural Networks*, CDF Note 6802.

- [6] Jet correction documentation:  
<http://www-cdf.fnal.gov/internal/physics/top/jets/corrections.html>
- [7] Robin Erbacher, Richard Hughes, Radu Marginean, Rob Roser, Evelyn Thomson, Brian Winer John Conway, *Measurement of the  $t\bar{t}$  Cross Section using Kinematic Variables*, CDF Note 6802.
- [8] Robin Erbacher, Richard Hughes, Radu Marginean, Rob Roser, Evelyn Thomson, Brian Winer John Conway, *Measurement of the  $t\bar{t}$  Cross Section using Kinematic Variables*, CDF Note 6206.
- [9] V. Drollinger, M. Gold, J. Jarrell, V. Rekovic, D. Smirnov, *A Neural Network Measurement of the  $t\bar{t}$  Pair Production Cross Section in the Lepton+Jets Channel*, CDF Note 6078.
- [10] Eric Moore, Michael Gold, Steve Worm, *A Neural Network Measurement of the top-antitop cross section in lepton+jets*, CDF Note 5796.
- [11] Robin Erbacher, *et al.*,  *$t\bar{t}$  Event Selection and Signal Acceptance of the Winter 2005 Lepton+Jets Sample*, CDF Note 7372.
- [12] Top Properties Page  
<http://www-cdf.fnal.gov/internal/physics/top/RunIITopProp/>
- [13] DQM good run list page  
<http://www-cdf.fnal.gov/internal/dqm/goodrun/good.html>
- [14] S. Jindariani *et al.*,  *$t\bar{t}$  Luminosity Uncertainty for Run2 up until August 2004*, CDF Note 7446.
- [15] Information on MC samples can be found here  
<http://www-cdf.fnal.gov/internal/physics/top/RunIIMC/topmc6/index.shtml>
- [16] Carsten Peterson, Thorsteinn Rongnvaldsson, Leif Lonnblad, *JETNET 3.0 - A Versatile Artificial Neural Network Package*, CERN-TH 7135/95.
- [17] Catalin Ciobanu, Richard Hughes, Phillip Koehn, Christopher Neu, Brian Winer, *A ROOT Interface to JETNET*, CDF Note 5434.
- [18] Stephen J. Roberts and Will Penny, *Neural networks: friends or foes?*, Sensor Review 17, 64 (1997).
- [19] A description of the procedure and the code can be found here  
[http://cdfrh0.grid.umich.edu/~miller/pdf/pdf\\_acceptance.html](http://cdfrh0.grid.umich.edu/~miller/pdf/pdf_acceptance.html)
- [20] A description of the procedure and the code can be found here  
[http://www-cdf.fnal.gov/internal/physics/joint\\_physics/instructions/zvrew.html](http://www-cdf.fnal.gov/internal/physics/joint_physics/instructions/zvrew.html)
- [21] Information on the JPScaleFactor class can be found here  
[http://www-cdf.fnal.gov/internal/physics/joint\\_physics/instructions/JPScaleFactor](http://www-cdf.fnal.gov/internal/physics/joint_physics/instructions/JPScaleFactor)
- [22] Information on the Perfidia method can be found here  
<http://ncdf70.fnal.gov:8001/PerfIDia/PerfIDia.html>
- [23] John Conway, David Cox, Robin Erbacher, Andrew Ivanov, Will Johnson, Alison Lister, Tom Schwarz *Search for Heavy Top  $t' \rightarrow Wq$  in Lepton Plus Jets Events in  $\int \mathcal{L} dt = 2.3 \text{ fb}^{-1}$* , CDF Note 9209.